Liquid metal embrittlement of molybdenum by the eutectic gallium-indium-tin alloy

T. Auger [a,*], S. Baiz [a], L. Bataillou [b], A. Klochko [b]

[a] *PIMM/Arts et Metiers Institute of Technology, CNRS, CNAM, UMR CNRS 8006, HESAM University, 151 boulevard de l'hôpital, Paris 75013, France*
[b] *Airthium SAS, Accelair, 1 chemin de la Porte des Loges, Les Loges-en- Josas 78350, France*

ARTICLE INFO

ABSTRACT

The liquid metal embrittlement (LME) sensitivity of pure molybdenum in liquid eutectic gallium-indium-tin alloy has been studied as a function of temperature by axisymmetric notched tensile testing. Molybdenum is an intrinsically brittle material that recovers a ductile fracture behavior above a transition temperature found in this study at 197 °C. The sensitivity of this refractory material to LME is demonstrated in the temperature range where it normally recovers ductile fracture (200–350 °C). The LME fracture mode is then a mixture of cleavage and intergranular cracking with no striking fractographic differences with intrinsic brittleness. This is the first case of LME at low temperature for a refractory material.

1. Introduction

Liquid metal embrittlement (LME) investigations have traditionally been divided between the study of the effect of the adsorption of a low melting point liquid metal on the mechanical properties of structural materials (typically a steel in contact with a liquid metal) and the study of LME model systems such as Al/Ga, Ni/Bi or Cu/Bi couples [1]. In the latter case, one does indeed study the interplay between LME and the spontaneous replacement of the grain boundary by an atomically thin "liquid-like" layer [2]. However, LME is for a majority of cases, to be understood as a change in the fracture mode (ductile to brittle) induced by the adsorption of the liquid metal during mechanical strain loading. It is indeed not demonstrated that intergranular cracking is systematically preceded by a grain boundary infiltration step in cases other than grain boundary wetting model systems so that it is still relevant to differentiate these two classes. There has been comparatively fewer studies on couples where one does not necessarily observe fast intergranular invasion like the afore mentioned LME model systems or those neglected by liquid metal cooling system's integrators. In this respect refractory materials such as molybdenum are almost a virgin and unexplored area in the field even relative to intrinsic sensitivity to LME. It is one of the main purposes of this article to fill the current gap in the couples that have been under scrutiny for LME.

Another interesting point for this system is that molybdenum has an intrinsic brittle fracture mode that transition to a ductile fracture mode at room temperature or slightly higher. It is therefore interesting to look at the interplay between the brittle fracture mode at low temperature

and the environmentally induced brittle cracking. In particular, one is interested into the similarities or differences between intrinsic brittle behavior and environment induced brittle behavior.

The present knowledge about the interaction of a liquid metal with the refractory metal molybdenum can be quickly summarized. The corrosive action of liquid tin on molybdenum has been studied in static exposure setup [3] where it was shown that the well-known effect of grain boundary grooving [4] can be observed in this system at 1250 °C. However, neither grain boundary diffusion nor liquid metal grain boundary penetration was found to occur. A model system for this latter behavior is the Mo/Ni system. It was studied at the atomic scale by transmission electron microscopy (HRTEM and HAADF) and a wetting Ni bilayer was observed on a general grain boundary after long term exposure to diffusion bonded nickel on molybdenum at 1350 °C [5–7] or annealing of dilute Mo(Ni) alloys at 1495 °C [8]. Grain boundary wetting (i.e., the existence of a thermodynamic driving force for spontaneous grain boundary wetting) or a concurrent process, grain boundary diffusion, was also investigated on Mo/Pb but no such behaviors were found neither at 700 °C nor at 1250 °C [9,3]. This illustrates that grain boundary wetting is system specific and to be evaluated on a case by case basis. The Mo/Pb system was also tested for its LME sensitivity at 700 °C with no observed detrimental effect of lead at such temperature [9]. The interaction of liquid gallium on molybdenum for compatibility as a container material has been studied but only from the point of view of corrosion. It is considered that up to a temperature of 400 °C, the interaction of gallium on molybdenum is limited such that it is a suitable container material below this maximum temperature [10]. At last, liquid plutonium (alloyed with gallium, Pu-1wt%Ga) is known to severely
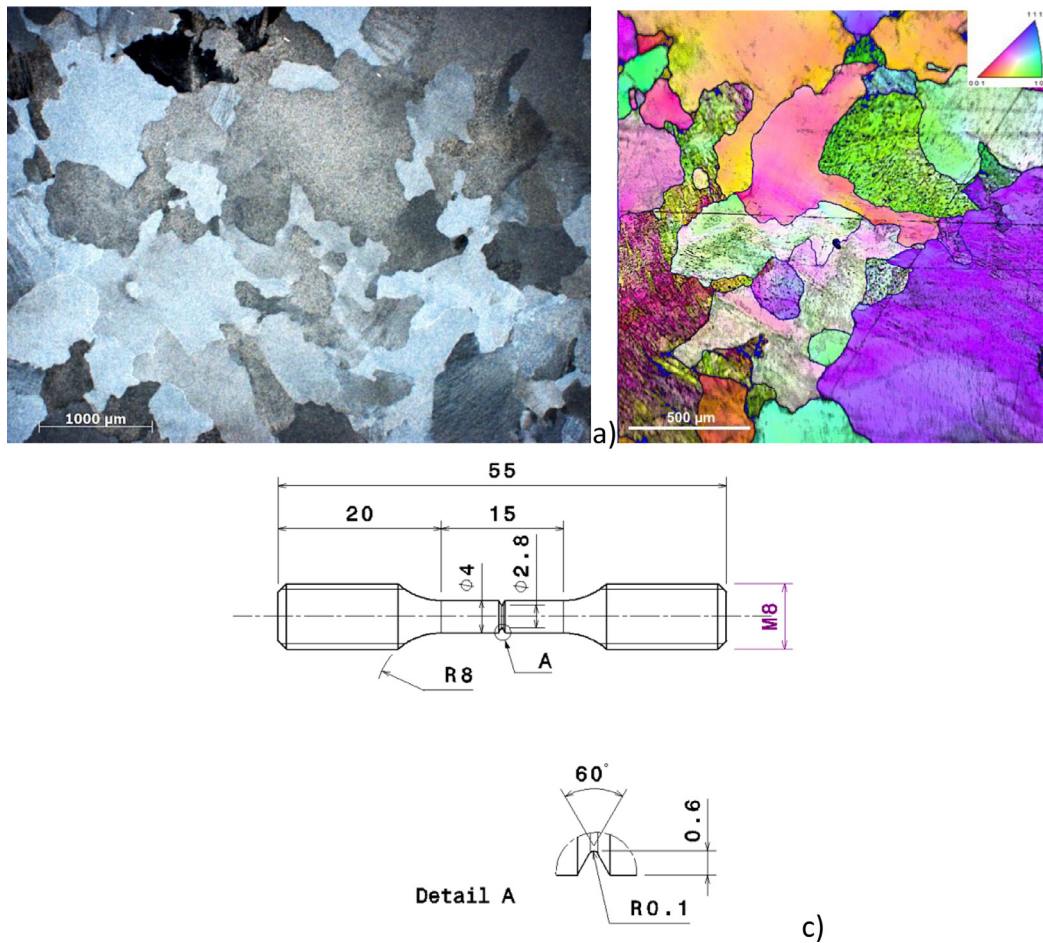
Fig. 1. (a) molybdenum microstructure as revealed using the Murakami reagent (optical dark field view, x5). (B) Inverse pole figure (IPF) maps of the initial molybdenum microstructure (c) Schematic of the tensile specimen.

embrittle molybdenum in tensile tests at 900 °C with essentially no plastic deformation and an intergranular fracture mode [11]. The fracture mode for this couple is reported as a typical example of an intergranular stress-corrosion cracking case. There is of course the unanswered question of whether the embrittlement is triggered by plutonium or whether it stems from the tiny gallium addition.

This short review of the effect of a liquid metal on molybdenum's mechanical behavior and corrosion resistance shows that the entire set of data was obtained at rather high temperature (700 °C and above) and is mostly concentrated on the grain boundary wetting issue. None of the available studies investigated LME's sensitivity in the sense of a change in fracture mode at lower temperature typical of low melting point liquid metals. The question of a potential sensitivity of molybdenum to LME at low temperature is therefore addressed for the first time in the work reported here where pure molybdenum has been mechanically tested in contact with Galinstan, the eutectic alloy of the gallium-indium-tin ternary system (69 wt% Ga, 21 wt% In, and 10 wt% Sn). The Galinstan alloy has two major advantages for this study. It has a melting point below room temperature (284 K/11 °C) and at the same time, the vapor pressure of this alloy is extremely low up to high temperature ($< 10^{-6}$ Pa at 500 °C). Overall this makes this liquid metal well suited for LME studies from room temperature up to 500 °C without the potential safety hazards found with other options (Hg or Na-K alloy).

2. Experimental procedures

The molybdenum used for this study was procured from Goodfellow in a bar format of 10 mm diameter. The stated purity level was 99.9%. Because the ductile to brittle transition temperature (DBTT) of molybdenum is sensitive upon metallurgical factors such as the interstitial impurities content [12,13], an analysis of the interstitial content (C, N, O) was carried out by interstitial gas analysis (IGA) of fused samples. Conversely, the main metalloid impurities content was characterized by glow discharge mass spectroscopy (GDMS). The composition is given in the table below.

The material was used in the as-received state. The mean grain size was characterized by optical micrography. The microstructure was revealed using the Murakami reagent on mirror polished material (10 g potassium ferrocyanide and 10 g sodium hydroxide for 100 ml distilled water). The results are shown in Fig. 1a: the main grain size was measured at about 500 μm.

An Electron BackScattered Diffraction (EBSD) map was measured on the initial state (Preparatin: SiC paper grinding + diamond down to 1 μm polishing followed by an ultrasonic vibration in a silica solution for 8 h. Mapping at 15 KeV with a step of 2 μm). The EBSD map revealed the partially recrystallized state of the bar with a significant fraction of the grains that still have large internal misorientation. Notched axisymmetric tensile specimens were machined from the bar using tungsten carbide machining tools (gripping of the sample was via screw threads). The diameter of the gauge length was 4 mm for a length of 15 mm. A transverse 60° notch of 600 μm depth for a tip radius of the order of 100 μm was machined at mid-gauge length (see Fig. 1b). The samples were used in the as machined state and neither surface polishing nor surface stress relief heat treatment were carried out. High purity gallium (99,999%), indium (999,995%) and tin (99,999%) were procured from Alfa Aesar. The eutectic Galinstan was obtained by amalgamation of indium and tin in liquid gallium heated slightly above room temperature.

Since molybdenum/Galinstan has not yet been reported as a LME couple, the search for a possible LME sensitivity should investigate at the same time wettability of the solid material by the liquid metal and carry out tests in a sufficiently wide range of kinetic conditions (such as temperature or strain rate in mechanical tests conditions) so as to ensure the LME domain is undoubtedly met. Indeed, depending on the metallurgical state (hardening, precipitation state, etc.) some changes in the kinetic domain may occur and LME may not be met experimentally. The wettability by Galinstan and a wide enough exploration of the temperature of the test (a kinetic factor) was explored here.

The deposit of small Galinstan drops on mirror polished molybdenum surfaces showed that it does not readily wet its surface (at room temperature). It is customary in these circumstances to proceed to a pre-wetting step in order to ensure this key requirement for LME sensitivity assessment. Wetting using a chemical etching treatment was first pursued, a process that works well with liquid mercury on austenitic steels [14]. Solutions of nitric acid and hydrochloric acid of various concentrations, known to be able to etch molybdenum, were used. It was however found that this wetting technique fails to promote an efficient wetting particularly at the rugged area of the notch of the sample. To replace the chemical etching technique, the process of ultrasonic wetting was applied. This wetting technique was in use back in the sixties [15] but it has been largely forgotten since and is disused today. To our knowledge, this is its first application within the LME research field in decades. It relies on the use of ultrasonic waves generated at high frequency (here 40 kHz) with a power flow well over 100 W.cm^{-2} (an empirical figure of the required power level). The generator used in this work was the LPX© welding module from the supplier Branson featuring a maximum power input of 550 W. The ultrasonic wetting process uses the cavitation regime at solid-liquid interfaces. The native oxide at the surface is etched during the collapse of cavitation bubbles generated by the ultrasonic wave [15]. The cavitation bubbles generated by the ultrasonic treatment are assumed to have no impact on the metallurgical state of the samples beyond the extreme surface. Practically, the horn (with a flat rectangular end geometry of 4 cm^2) was first wetted by the liquid metal by digging the flat end into a Galinstan reservoir. Then the tip of the horn was put in contact with the notched part at the maximum available power level. A correct wetting with this procedure was almost immediately achieved: an adherent film wets over the notched area of the sample and the close part of the gauge length. It is to be noted that a zero or a small macroscopic wetting angle is achieved in his way with the molybdenum/Galinstan system. The Mo/Galinstan system shows a nearly total wetting behavior.

The mechanical tests of wetted and reference samples were carried out in a glove box filled with argon gas (the setup is described in details in [16]). The kinetic factor was sampled by testing at various temperature. This was carried out by the internal heating technique (Joule effect) on an isolated high intensity current loop in serial link with the sample. The temperature was measured at the notch level via a thermocouple mechanically pressed on the surface at the notch level. A monitoring of the temperature was also carried out by pyrometry above 50 °C (PbS detectors with a sensibility range either from 50 to 400 °C or 160 to 1250 °C – Lumisense provider). The sample can be mechanically loaded via a MTS 20/H uniaxial testing machine connected via feedthrough to the glove box. An online purification process allows to keep dioxygen and water vapor contents to concentrations lower than 1 ppm each during testing. This low level of gas contamination is indeed necessary to avoid spurious surface oxidation of the liquid melt during mechanical testing. The test is conducted first with a pre-heating step up to the test temperature during which thermal equilibration is achieved after a typical delay between half an hour and one hour. Then mechanical loading is started with a constant crosshead speed set here to 1.66 μm.s^{-1}. The temperature is maintained at the set value during mechanical straining by a feedback loop with the injected power. For each temperature, a reference sample and a Galinstan wetted sample are tested at the same cross-head speed for comparison. The force-displacement curve is inte-
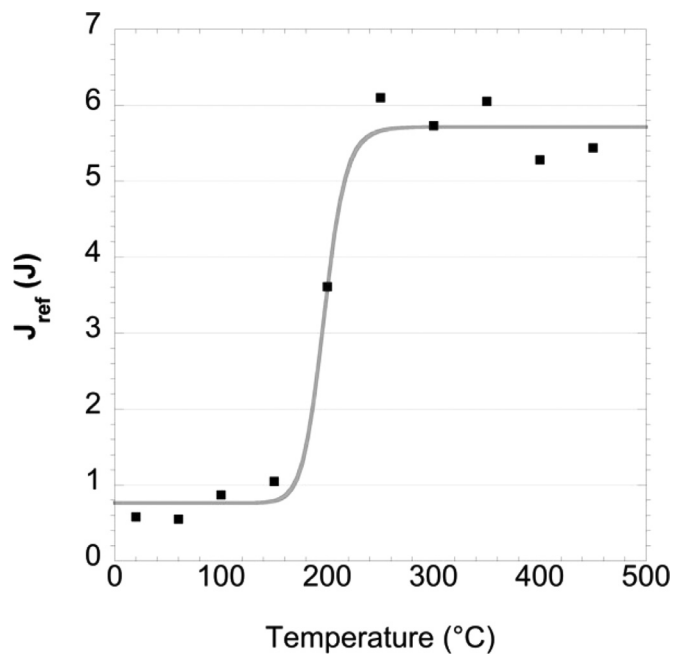

Fig. 2. energy to fracture as a function of temperature for reference Mo notched axisymmetric tensile specimens. The data fit by a sigmoid is shown in gray (R^2 score of 0.986).

grated to provide a measurement of the energy to fracture (in Joule) for each specimen. Any LME behavior can be evidenced by calculating the ratio of the energy to fracture in contact with Galinstan with the energy to fracture of the reference condition. Such an indicator gives a quantitative gauge of the LME sensitivity domain well suited to the notched axisymmetric test geometry [17].

After testing, the fracture surfaces are covered by Galinstan because capillarity supplies the liquid at the crack front during crack propagation (not necessarily in phase with the crack front expansion through, this point will be further assessed in discussion). In order to prepare samples for scanning electron microscopy (SEM), the sample's tip is dug into a reservoir of pure liquid mercury for at least one hour. Gallium, indium and tin are miscible with liquid mercury up to a few atomic percents such that the molybdenum-Galinstan interface is (a priori) essentially replaced by a molybdenum-mercury one by amalgamation. Then the sample is cleaned using ultrasonic cleaning in a distilled water bath (the surface tension of mercury is lower than the one of Galinstan so that the free surface is easier to break into small droplets). A few iterations of cleansing with the ultrasonic bath are sufficient to remove entirely the liquid amalgamated mercury solvent from the fracture surface. The fractographic analysis was carried out in a Zeiss tungsten SEM (EVO MA10). Transverse cut of LME fractured molybdenum sample were prepared by diamond wire saw cut. The surface was mirror polished using up to 1 μm size diamond paste and etched using the Murakami chemical reagent (exposure time of 30 s to 1 min). The observation of the crack path was then conducted using an optical microscope.

3. Results

3.1. Mechanical tests

The mechanical response to a monotonic loading of bulk molybdenum in the notched geometry can be best represented by the energy to fracture in Joule (unnormalized tensile toughness). It can be used to discuss qualitatively the mechanical behavior of our material. The results of the reference tests are reported using this quantity from room temperature up to 450 °C in Fig. 2. The mechanical behavior shows an energy to fracture between 0.6 and 1 J up to 200 °C (lower shelf energy) where
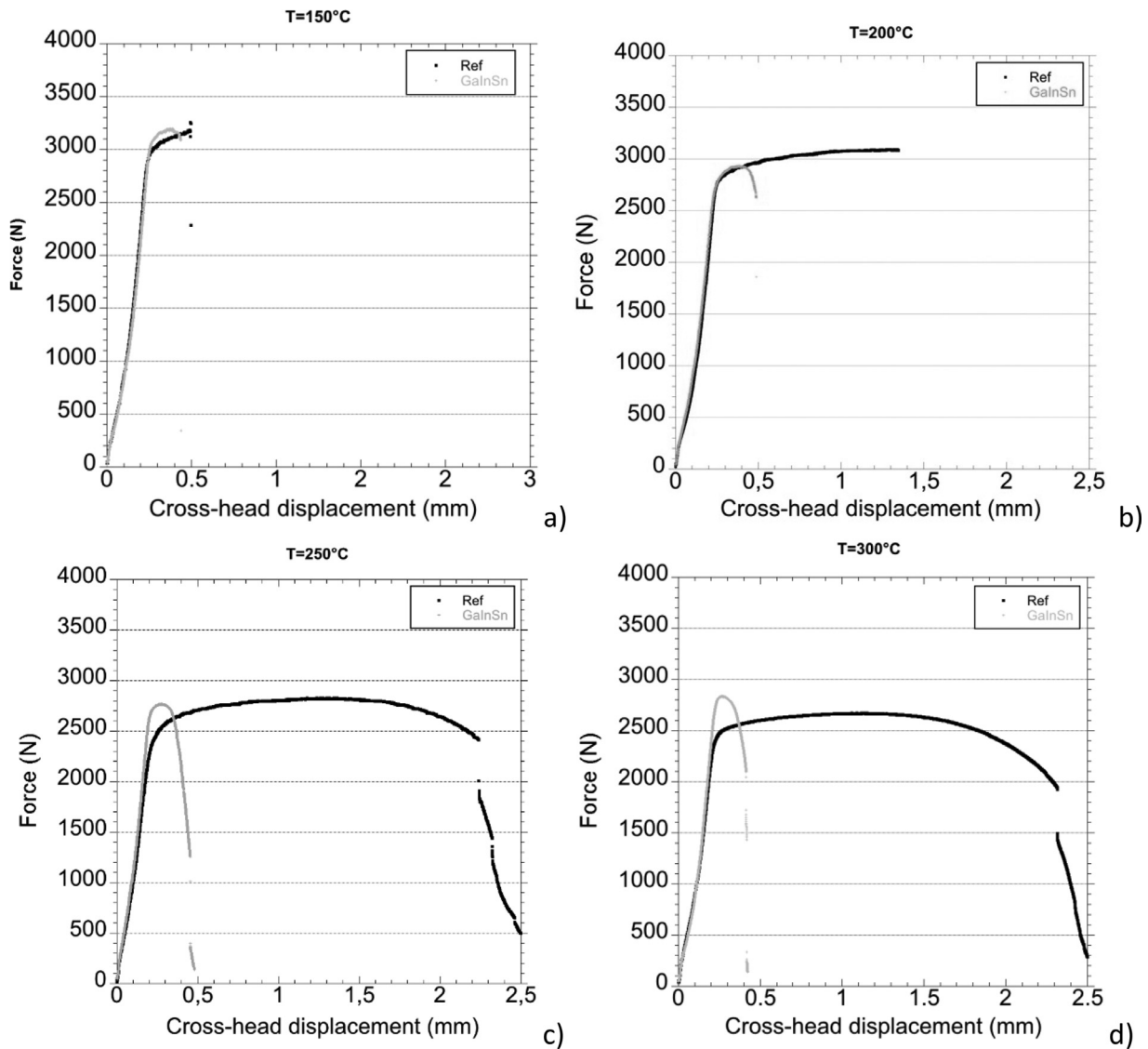
Fig. 3. Force vs. cross-head curves at the temperature of 150 °C (a) 200 °C (b) 250 °C (c) and 300 °C (b) for reference and Ga-In-Sn wetted Mo notched axisymmetric tensile specimens (crosshead speed of 0.1 mm.min^{-1}).

it suddenly increases to upper shelf energies (between 5 and 6 J) above this transition temperature. A sigmoid curve fitted to the data points allows to determine the DBTT at 50% of the plateau value. The transition temperature is then found at 197 °C ($R^2 = 0.986$). Therefore, there is a very sharp brittle to ductile transition with temperature for fracture as expected for the bcc intrinsically brittle molybdenum.

The mechanical behavior of molybdenum in the temperature range for brittleness consists into an elastic strain part up to the yield point. This is followed by a strain hardening phase before brittle fracture suddenly sets in (except at room temperature where fracture precedes the onset of plasticity). Because of the notched geometry and the plastic strain localization it induces, an assessment has not been carried out of the maximum levels of strain and stress reached in these tests at the notch before fracture. In the ductile recovery temperature range (between 200 and 300 °C), a significant strain hardening part is observed before ductile damage fully develops. At 350 °C and above, no strain hardening occurs since one observes a load drop immediately beyond the yield point. This is indicative of intense strain localization above 300 °C.

Typical force-crosshead displacement curves for a reference molybdenum and a Galinstan wetted specimen both carried out between 150

and 300 °C are shown in Fig. 3. For the reference sample, damage and then final fracture both occur beyond a maximum force loading (parented to the ultimate tensile stress). On the other hand, while in contact with Galinstan, LME cracks are initiated readily after the yield point, eventually initiating a crack propagation outside the notched area (this explains why the maximum force can sometimes be higher than one would expect if the onset of plasticity was located at the notch area only; this is clearly the case at 250 °C as shown in Fig. 3c). The onset of cracking occurs close to the yield point that is indicative of a very strong embrittlement by the liquid metal. One note that at 150 °C, there is mechanically no difference. Since it is difficult to ensure, first that the ultrasonic wetting process has achieved a uniform wetting condition in the cylindrically curved notch and, second that other areas than the notch are not wetted by Galinstan, one may not avoid the case where crack initiation also potentially appears at the gauge level of the sample. This is bound to give a tortuous crack propagation path and an extra-added contribution to the energy to fracture. This was visibly the case for some tests but it was not accounted for in the calculation of energy to fracture due to its estimated small effect.

At low temperature, in the intrinsically brittle fracture temperature range, the crack initiates at the notch level and is followed by a very fast
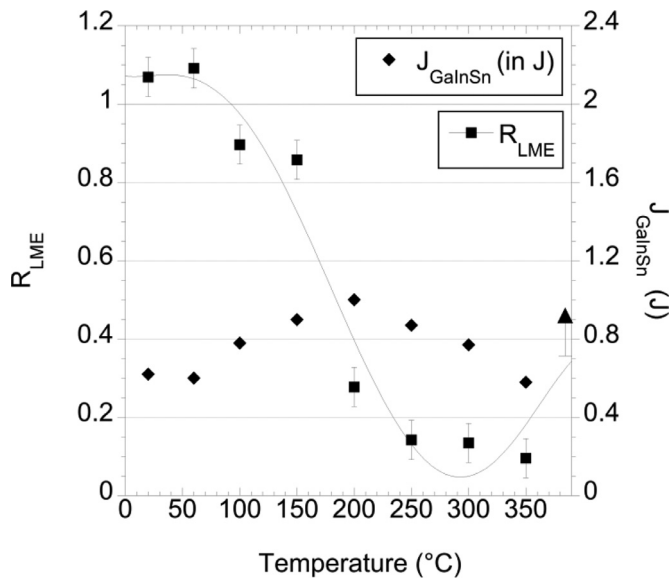
Fig. 4. (Left scale) R_{LME} ratio of the energy to fracture in contact with Galinstan with the energy to fracture of the reference sample as a function of test temperature (the line is a guide). The arrow at 400 °C is only indicative and is higher than measured (the crack did not initiate at the notch level). (Right scale) Data of the energy to fracture in contact with Galinstan (J_{GaInSn}) are plotted in Joule.

critical crack propagation right after yielding or slightly after. This is observed for all specimen (wetted and reference). The total crack propagation in the notched section of 2.8 mm diameter takes place within one or two clock ticks of the mechanical test machine sampling frequency (10 Hz) which gives a lower bound for the crack speed of 0.014 m.s^{-1}. It is likely that the crack speed is much higher given the loud noise at fracture from the brutal release of stored elastic energy.

When the tests are carried out at intermediate temperatures (for this study between 200 and 350 °C), the crack propagation proceeds subcritically for the Galinstan wetted specimens. In such conditions, the measurement of the energy to fracture can be relied upon without caution. The total time at all temperatures for the load to drop by a factor of two from the onset of a regular crack propagation is of the order of one minute (data spreads from 65 to 70 s). Given the sample geometry, the estimate of the order of magnitude of the LME sub-critical crack propagation speed is then of the order of 10 μm.s^{-1}.

When testing above 350 °C in contact with Galinstan (at 400 and 450 °C), the main LME crack initiated outside the notched area. The heating process during our test procedure generates some temperature gradient along the gauge length of the sample itself. The center is heated at a slightly higher temperature than the areas close to the sample threads due to the section reduction. On those samples, crack initiation occurred outside the notch area at the gauge level. This can be rationalized by the fact that at such temperature, a ductility recovery process makes it impossible to initiate at the hotter notch level while it can still suffer from a strong embrittlement in the lower temperature part of the gauge length that are still exposed to Galinstan (an outcome of covering a large area by the ultrasonic wetting procedure). Being a systematic effect, these tests at 400 and 450 °C have therefore been discarded from further analysis. One may say qualitatively that some ductile recovery occurs above 400 °C for the liquid metal induced embrittlement.

The LME sensitivity is assessed by the ratio of the energies to fracture R_{LME} (wetted by Galinstan versus reference one). The results are displayed in Fig. 4 as a function of test temperature up to 350 °C only due to the limitation just mentioned above.

According to Fig. 4, one does observe that in the room temperature range for brittle fracture, the LME sensitivity is small or not measurable in this geometry ($R_{LME} \approx 1$). A drop reaching just around 15% in

fracture energy can be seen at 100 and 150 °C. Nevertheless, fracture proceeds in a brittle manner given the low energy to fracture measurement (see also the fractographic analysis). From 200 °C till 350 °C, the LME induced brittle fracture is very strong up to a drop of the order of 90% of the reference energy to fracture at 350 °C. The onset of the LME range coincides with the intrinsic ductility recovery of molybdenum and extends up to a recovery temperature near 400 °C. It is worthwhile to note that the energy to fracture does not vary by a large amount as a function of the temperature for the wetted specimens. This indicates a similar degree of embrittlement in the LME range than the intrinsic brittleness (Fig. 4, right scale) in spite of the tremendously slower LME crack speed compared with the very high intrinsic brittle crack speed. This is indicative of a very strong embrittlement.

3.2. Fractographic analysis

The low magnification SEM analysis is shown in Fig. 5. The brittle character of fracture of the reference material can be seen on all the fracture surfaces from room temperature to 200 °C ((a) to (c), 200 °C is within the transition range and final fracture is still brittle for reference). One can see that the fracture behavior for the reference molybdenum above 200 °C transition to a ductile fracture mode with a void growth and coalescence fracture mode (with still a few signs of intergranular decohesion, Fig. 5d). Such a behavior is consistent with a ductility recovery above the transition temperature (set at 197 °C in our analysis).

The fracture surface of Galinstan wetted specimen can be seen in Fig. 5e and f (corresponding to a test temperature of 200 and 300 °C). Liquid Galinstan clearly induces a brittle fracture instead of the standard ductile fracture mode. The fracture surface shows then typical cleavage type characteristics with cleavage rivers. At 300 °C, a coexistence of cleavage with an intergranular fracture mode is clear.

At higher magnifications for all the brittle cases of pure molybdenum, fracture is seen to occur mainly by cleavage with characteristic cleavage rivers (Fig. 6a). A contribution of intergranular cracking can also be noticed as well as limited cavity growth up to micrometric size (Fig. 6c). These cavities can be seen on a very small fraction of the fracture surface indicating that some plastic deformation can locally develop most likely at slip band intersections during the cracking process. Small scale view of the typical fracture surface of the LME condition can be seen in Fig. 6b for a crack initiation site and in Fig. 6d for the fracture surface away from the notch area. The similarities of the fracture surfaces in the brittle regime and the LME regime are striking (Fig. 6c and d: cleavage rivers, intergranular cracking and small cavities at some spots).

The transverse cut analysis of the molybdenum sample broken in GaInSn at 300 °C confirms that the fracture path is a mixture of intergranular cracks (Fig. 7a) and cleavage cracks (Fig. 7b). Crack branching is also induced by grain boundaries with either a deflection of the cleavage crack plane with a portion of the crack following a former grain boundary (See Fig. 7a). Some switch from a purely intergranular crack to a pure cleavage crack can also be observed (Fig. 7b). This confirms the analysis of LME at 300 °C carried out on the fracture surface shown in Fig. 5f.

4. Discussion

One can compare the ductile to brittle temperature transition (DBTT) for molybdenum found in our study to those found in earlier studies. Pure and ultra-high purity molybdenum have a transition temperature decreasing with purity to lower than room temperature in several studies [18–20]. Conversely, it is known that impurities, heat treatment and coarse grain size have a major influence in raising the transition temperature above the ambient one [20]. For example, a transition at 375 K (102 °C) was found on industrial coarse-grained molybdenum [21] while a much lower transition temperature of 243 K (–30 °C) was found for ultra-pure molybdenum [18]. The transition temperature found in our
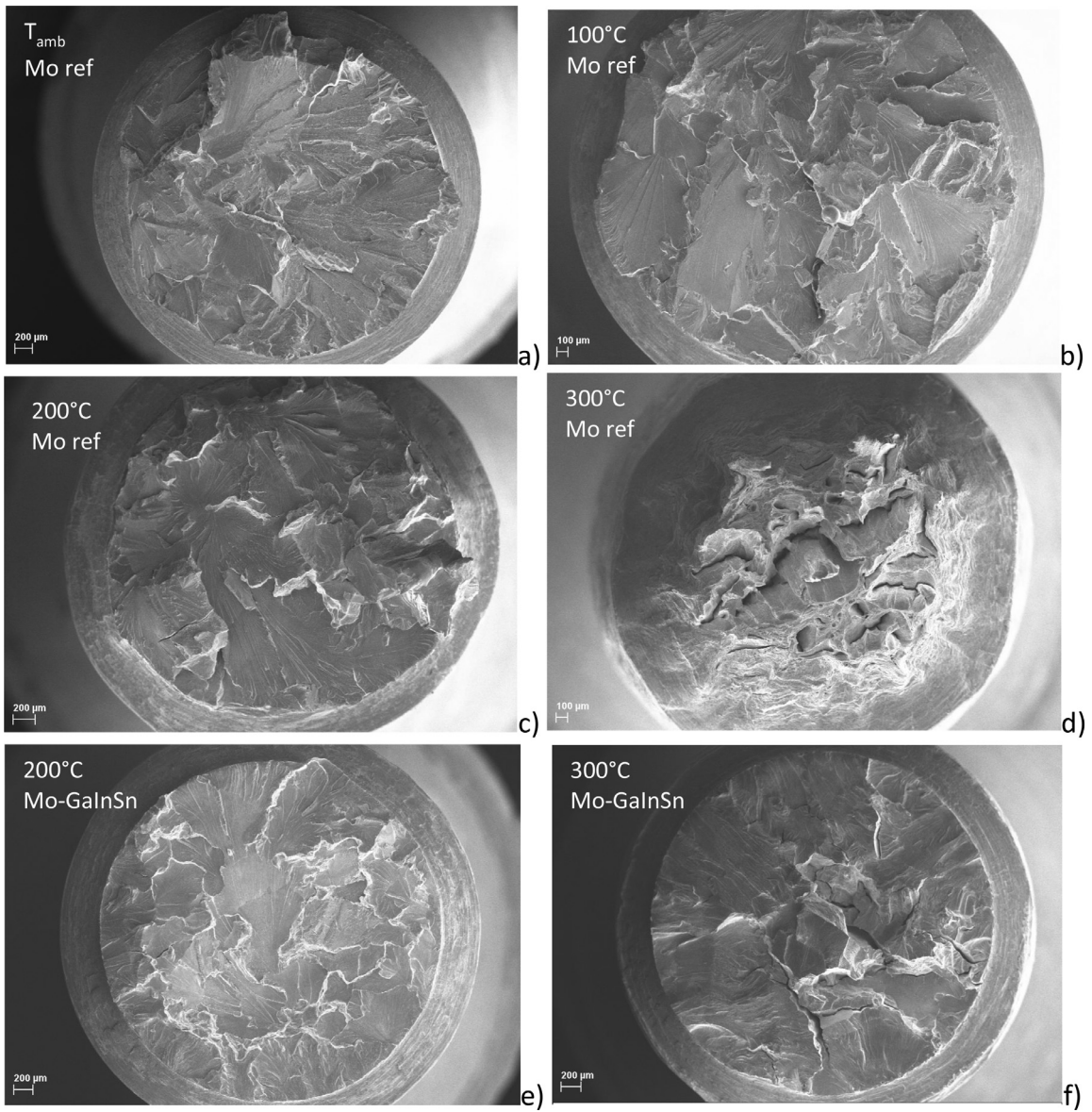
Fig. 5. SEM analysis of Mo fracture (a) room temperature, (b) 100 °C, (c) and (e) 200 °C, (d) and (f) 300 °C. (e) and (f) show the Mo-Galinstan fracture surface at 200 °C and 300 °C, respectively.

Table 1
impurities content of molybdenum (remainder is Mo).

	C	O	N	W	Ni	Fe	Cr	K	Co	Ca	Cu	S	Ba	Si	Mn	Ti	B,Mg,Al,P,Sc,V,Mn Zn,Ga,In,Sn,Pb,Bi
Content (wt ppm)	92	105	15	45	15	14	14	14	8.1	3	2.5	2.4	2.4	2.4	1.2	<5	<1
Analysis technique	IGA			GDMS													

study for our molybdenum is however even higher than those found in these studies. The effect of test's strain rate is important and can be non-negligible with a clear trend towards higher transition temperature as the strain rate is increased (more or less + 50 K with a hundred-fold strain rate increase) [13,22,23]. The strain rate used in this study is however in the low range of these studies and strain rate effects are insufficient by themselves to explain the high value of DBTT of the material used here. The interstitials content analysis (see Table 1) shows that the molybdenum used in this study had higher oxygen and carbon content than zone purified materials, sufficient to significantly raise the DBTT threshold as shown in previous studies [12]. Another contribu-

tion may lay into the geometry used in this work. It has been shown by Cockeram and Chan [24] that the triaxiality of the loading strongly influences the measured DBTT: shifting from a tensile test geometry to a fracture toughness geometry, it increases from 25 °C up to 200 °C for a low-carbon arc-cast (LCAC) molybdenum. Because of the high triax-ility at the notch in our geometry, a significant increase of the DBTT is indeed to be expected compared with what would be measured in a tensile test geometry. An indication that this effect is probably domi-nant over the influence of impurities comes from the fact that while the interstitials content of our specimen is two times higher than in this for-mer study, the measured DBTTs are similar (150 °C for LT orientation
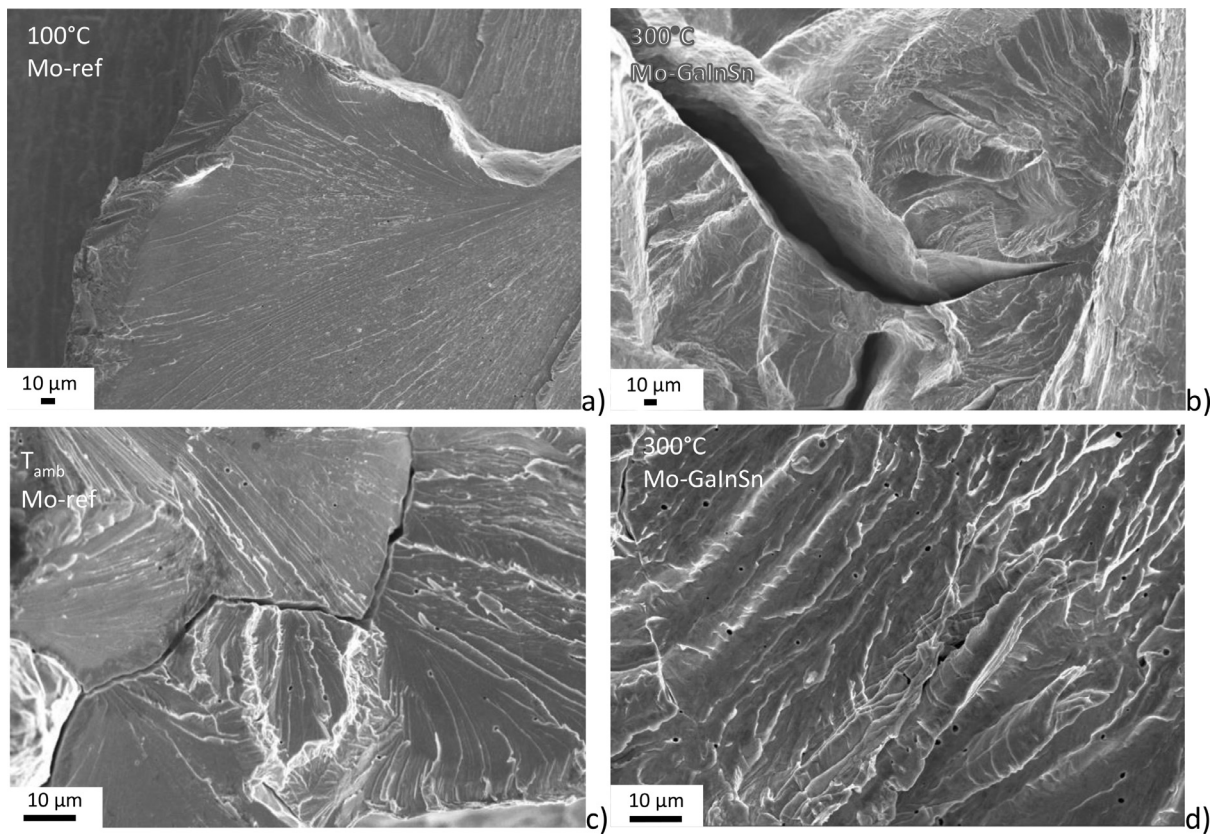
Fig. 6. SEM fractography of fracture surfaces: (a) Initiation site of reference molybdenum at 100 ˚C (b) Initiation site of Galinstan wetted molybdenum at 300 ˚C (c) Molybdenum reference at room temperature (d) Molybdenum-Galinstan at 300 ˚C.
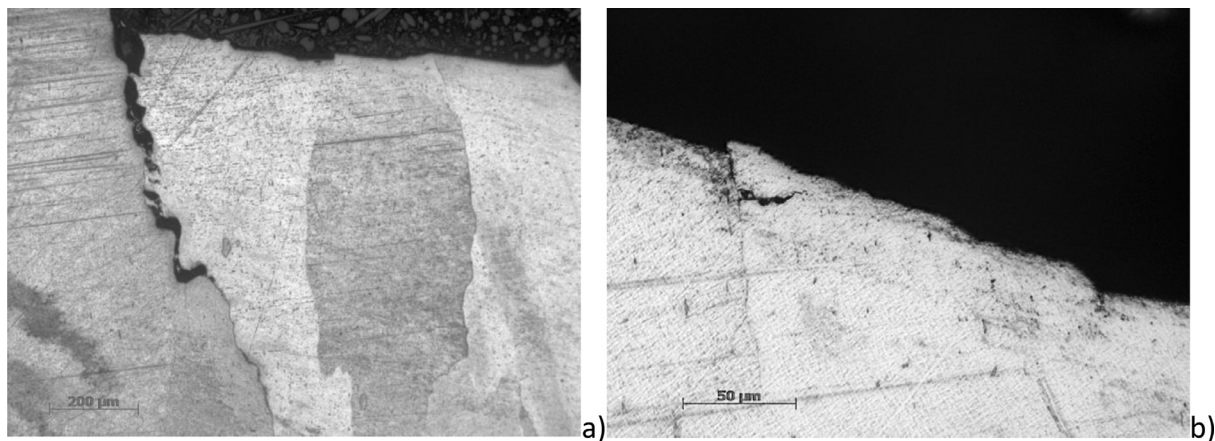

Fig. 7. Optical microscopy of transverse cut of the Mo-GaInSn sample at 300 ˚C. (a) X10 magnification view of the area next to the fracture surface (b) x50 view of a small switch from intergranular to cleavage area (color online).

and 200 ˚C for TL orientation in [24]). Overall, this high shift of DBTT induces a significant effect on the LME temperature survey by reducing the ductile fracture temperature range. While it does not affect the LME intrinsic sensitivity assessment past the DBTT, it is representative of the variability induced by the mechanical testing geometry.

For test temperatures below 200 ˚C, a high crack speed is observed during the brittle final fracture of both reference tests and Galinstan-wetted tests. It is customary in brittle fracture to observe that the maximum crack front propagation rate is some fraction of the Rayleigh wave velocity (between 0.4 to 0.6 $V_{Rayleigh}$ for tungsten monocrystals [25]). In these circumstances, it is difficult to think that the crack propagation can be controlled by the liquid adsorption owing to the dif-

ficulty of the liquid to follow such a fast propagating crack front by capillarity. In these dynamic conditions, the capillary fluid flow should become inertial and should reach a limiting speed creating a lag between the opening crack front and the flowing liquid. This limiting speed for capillary flow can be estimated by the following dimensional relationship: $V_{capillary} = \gamma_{GaInSn}/\eta_{GaInSn}$ which reads the liquid speed $V_{capillary} = 222.5$ m.s^{-1}, with the surface tension $\gamma_{GaInSn} = 534$ mN.m^{-1} and the viscosity $\eta_{GaInSn} = 2.4$ mN.s.m^{-2} [26,27]. A brittle crack front propagation at full speed i.e., a fraction of the Rayleigh wave velocity as mentioned earlier ($0.4 \times 6190 = 2476$ m.s^{-1}) may then be an order of magnitude too high to enable the required LME condition of a wetted crack tip. This is therefore likely to induce a lack of liquid metal adsorp-

tion at the critical fracture site then rationalizing that no (or limited) LME is observed until molybdenum ceases to fracture by a brittle mode. It would be interesting to test further the transition temperature with an interstitial free molybdenum showing a lower DBTT (this is left for future work).

The LME sensitivity of notched molybdenum has been studied in contact with Galinstan in a wide temperature range (RT to 450 ℃). As the tested molybdenum (99.9% purity) normally fails in a brittle mode from the room temperature up to 200 ℃ with a high crack speed, the liquid metal adsorption has a null or a small effect on the already brittle fracture process. It therefore seems difficult, at least in our notched geometry, to assess concurrent fracture processes (between the intrinsic brittle fracture and the adsorption induced fracture for example unlike what was achieved on brittle silicon with the adsorption of dioxygen via the gas phase [28]). Testing quantitatively a Griffith type cleavage fracture mechanism where liquid metal adsorption induces a surface energy reduction is unfortunately not possible in this geometry with such a high DBTT material. It remains to be shown that molybdenum can be embrittled at low temperature, this could be possible studied using high purity material with a lower DBTT.

At higher temperature, a strong LME phenomenon is observed in this system from 200 to 350 ℃ whereas otherwise unwetted molybdenum shows a ductile recovery. The contact with liquid Galinstan extends therefore the brittle fracture range up to 350 ℃. Beyond this temperature, the experimental apparatus with Joule effect heating prevents a correct crack initiation at the notch jeopardizing consistent measurement. Instead, cracks initiate in lower temperature areas of the sample outside the notch. This however implies qualitatively the onset of a ductile recovery above 350 ℃. This upper temperature is also correlated with the onset of dewetting of the Galinstan film. Indeed, the formation of large wetting angle drops could be observed visually in the course of testing. This would indicate that the intimate contact condition can no longer be maintained at the interface above such transition temperature. The mechanical behavior of pure molybdenum not being known for a drastic change at these temperatures, the ductile recovery mechanism can then be equally ascribed to the onset of liquid metal desorption or to a change in wettability. An influence of a potential corrosion concern due to oxygen impurity can't be excluded neither. At room temperature, the solubility of oxygen in gallium or indium is extremely low but reaches ppm levels above 500 ℃ [29]. Overall LME is observed over a temperature interval of 150 ℃. This is not surprising since such a ductility trough is found in many LME systems [30].

The crack propagation in the LME range is subcritical with an estimated crack speed of the order of 10 μm.s^{-1}. The slow kinetics of such a LME crack contrasts with the low energy to fracture that remains of the order of the one of intrinsic brittle fracture of molybdenum. At the same time, fracture surfaces of brittle and LME induced fracture look alike at small scale indicating that cleavage is the dominant fracture mode in both cases. In terms of LME mechanism, it could indicate that adsorption induced fracture is a viable mechanism for the couple Mo/GaIn. As the test temperature reaches 300 ℃, intergranular cracking becomes more prominent indicating that the issue of grain boundary wetting in Mo/Ga becomes more and more similar to the high temperature Mo/Ni intergranular wetting case [5–8]. We note that LME here occurs in a system (Mo/Ga) with at least four intermetallics phases. The requirement in LME of mutual immiscibility between the solid and the liquid is here completely misleading.

5. Conclusion

This study reveals a new case of LME in a system consisting of a refractory element with a low melting point liquid metal, a combination never tested before. One key element in the sample preparation procedure is the incorporation of an ultrasonic wetting procedure that allows to enforce in a simple way this essential requirement. LME behavior is observed within a large temperature range. This system has all the attributes of a classical LME system between 200 and 350 ℃. Brittle fracture at low temperature and FML induced brittle cracking share many post-mortem characteristics: there are not striking fractographic differences between intrinsic embrittlement and LME. Instead large difference in the crack speed transpire from a rough estimate. This case of embrittlement could probably be used as a model system for investigating LME cracking with the notable experimental advantages of witnessing subcritical fracture (provided that at least a geometry optimization would be carried out).

Declaration of Competing Interest

The authors declare that they have no known competing financial interests or personal relationships that could have appeared to influence the work reported in this paper.

Acknowledgments

References

[1] D.G. Kolman, A review of recent advances in the understanding of liquid metal embrittlement, Corrosion 75 (2019) 42–57.

[2] J. Luo, A short review of high-temperature wetting and complexion transitions with a critical assessment of their influence on liquid metal embrittlement and corrosion, Corrosion 72 (2016) 897–910.

[3] A. Charai, I. Kutcherinenko, J.M. Penisson, V. Pontikis, L. Priester, K. Wolski, T. Vystavel, Electron microscopy and auger spectroscopy study of the wetting of the grain boundaries in the systems Mo-Pb, Mo-Sn, Mo-Ni and Ni-Pb, J. Phys. IV 12 (2002) 277–287.

[4] W.W. Mullins, Two-dimensional motion of idealized grain boundaries, J. Appl. Phys. 28 (1957) 333–339.

[5] B.B. Straumal, V. Semenov, V. Glebovsky, W. Gust, Grain boundary wetting transition in the Mo-Ni system", Defect Diffus. Forum 143-147 (1996) 1517–1522.

[6] E. Rabkin, D. Weygand, B. Straumal, V. Semenov, W. Gust, Y. Brechet, Liquid film migration in a Mo(Ni) bicrystal, Philos. Mag. Lett. 73 (1996) 187–193.

[7] J.M. Pénisson, M. Bacia, T. Vystavel, Segregation, precipitation and wetting of tilt grain boundaries in molybdenum, Interface Sci. 12 (2004) 175–186.

[8] X. Shi, J. Luo, Developing grain boundary diagrams as a materials science tool: a case study of nickel-doped molybdenum, Phys. Rev. B 84 (2011) 014105.

[9] R.C. Asher, D. Davies, S.A. Beetham, Some observations on the compatibility of structural materials with molten lead, Corros. Sci. 17 (1977) 545–557.

[10] L.R. Kelman, W.D. Wilkinson, F.L. Yaggee, Resistance of Materials to Attack by Liquid Metals, Argonne National Laboratory, Chicago, Illinois, U.S., 1950 report ANL-4417, doi:10.2172/4419134.

[11] D.R. Lesuer, J.B. Bergin, S.A. McInturff & B.A. Kuhn, "Liquid-metal embrittlement of refractory metals by molten plutonium" , Annual technical meeting of the international metallographic society; Brighton; UK; 18-20 Aug 1980. (UCRL–83986). Lawrence Livermore National Lab. (1980) United States.

[12] A. Lawley, J. Van Den Sype, R. Maddin, Tensile Properties of zone-refined Molybdenum in the Temperature Range 4.2-373°K, J. Inst. Met. 91 (1962) 23–28 1963.

[13] N. Igata, K. Miyahara, H. Asanuma, The effect of carbon charge on the ductility of electron-beam melted molybdenum, J. Jpn. Inst. Met. 43 (1979) 1211–1212.

[14] L. Medina−Almazán, J.C. Rouchaud, T. Auger, D. Gorse, Optimization of contact conditions between iron base alloys and mercury at room temperature, J. Nucl. Mater. 375 (2008) 102–112.

[15] W. Rostoker, J.M. McCaughey, M. Markus (Eds.), Embrittlement by Liquid Metal, Editor Van Nostrand Reinhold, New York, U.S.A, 1960.

[16] B. Barkia, J.L. Courouau, E. Perrin, V. Lorentz, M. Rivollier, R. Robin, L. Nicolas, C. Cabet, T. Auger, Investigation of crack propagation resistance of 304L, 316L and 316L(N) austenitic steels in liquid sodium, J. Nucl. Mater. 507 (2018) 15–23.

[17] S. Hémery, T. Auger, J.L. Courouau, F. Balbaud-Célérier, S. Hémery, T. Auger, J.L. Courouau, F. Balbaud-Célérier, Effect of oxygen on liquid sodium embrittlement of T91 martensitic steel, Corros. Sci. 76 (2013) 441–452.

[18] E.M. Passmore, Correlation of temperature and grain size effects in the ductile-brittle transition of molybdenum, Philos. Mag. 111 (1965) 441–450.

[19] G.A. Sargent, B.J. Shaw, Stress relaxation and the ductile-brittle transition temperature of molybdenum, Acta Metall. 14 (1966) 909–9012.

[20] J.C. Thornley, A.S. Wronski, The effect of annealing on the ductile-brittle transition temperature of cast molybdenum of constant grain size, J. Less Common Met. 21 (1970) 205–211.

[21] Y. Hiraoka, H. Kurishita, M. Narui, H. Kayano, Fracture and ductile-to-brittle transition characteristics of molybdenum by impact and static bend tests, Mater. Trans. 36 (1995) 504–510 JIM.

[22] A.S. Wronski, A.C. Chilton, E.M. Capron, The ductile-brittle transition in polycrystalline molybdenum, Acta Metall. 17 (1969) 751–755.

[23] (Met. Soc. Conferences, Vol. 17) L.L. Seigle, C.D. Dickinson, M. Semchyshen, I. Perlmutter, Effect of mechanical and structural variables on the ductile-brittle transition

in refractory metals, in: Refractory Metals and Alloys II, Interscience Publishers, New York, 1963, p. 65. (Met. Soc. Conferences, Vol. 17).

[24] B.V. Cockeram, K.S. Chan, *In-Situ* fracture studies and modeling of the toughening mechanism present in wrought low-carbon arc-cast molybdenum, titanium-zirconium-molybdenum, and oxide-dispersion-strengthened molybdenum flat products, Metall. Mat. Trans. A 39 (2008) 2045–2067.

[25] D. Hull, P. Beardmore, Velocity of propagation of cleavage cracks in tungsten, Int. J. Fract. Mech. 2 (1966) 468–487.

[26] R.E. Clegg, Fluid flow based model to predict liquid metal induced embrittlement crack propagation rates, Eng. Fract. Mech. 68 (2001) 1777–1790.

[27] T. Liu, P. Sen, C.J. Kim, Characterization of nontoxic liquid-metal alloy Galinstan® for applications in microdevices, J. Microelectromech. Syst. 21 (2012) 443–450.

[28] M. Shaheen-Mualim, A. Gleizer, D. Sherman, Dynamic stress corrosion cracking in silicon crystal, Int. J. Fract. 219 (2019) 161–174.

[29] T. Narushima, D. Sajuti, K. Saeki, S. Yoshida, Y. Iguchi, Oxygen solubility in liquid gallium and liquid indium, J. Jpn Inst. Met. 59 (1995) 37–43.

[30] B. Joseph, M. Picat, F. Barbier, Liquid metal embrittlement: a state-of-the-art appraisal, Eur. Phys. J. Appl. Phys. 5 (1999) 19–31.